

# Interaction of Human Plasma Proteins with Thin Gelatin-Based Hydrogel Films: A QCM-D and ToF-SIMS Study

Sina M. S. Schönwälder,<sup>†</sup> Florence Bally,<sup>†,‡</sup> Lars Heinke,<sup>†</sup> Carlos Azucena,<sup>†</sup> Özgül D. Bulut,<sup>†</sup> Stefan Heißler,<sup>†</sup> Frank Kirschhöfer,<sup>†</sup> Tim P. Gebauer,<sup>§,||</sup> Axel T. Neffe,<sup>§,||</sup> Andreas Lendlein,<sup>§,||</sup> Gerald Brenner-Weiß,<sup>†</sup> Jörg Lahann,<sup>†</sup> Alexander Welle,<sup>†,⊥</sup> Jörg Overhage,<sup>†</sup> and Christof Wöll<sup>\*,†</sup>

<sup>†</sup>Karlsruhe Institute of Technology (KIT), Institute of Functional Interfaces (IFG), 76344 Eggenstein-Leopoldshafen, Germany

<sup>‡</sup>University of Upper Alsace (UHA), Institute of Materials Science of Mulhouse (IS2M, UMR 7361), 68093 Mulhouse, France

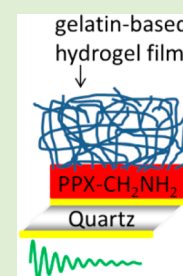
<sup>§</sup>Helmholtz-Zentrum Geesthacht, Institute of Biomaterial Science, 14513 Teltow, Germany

<sup>||</sup>Helmholtz Virtual Institute - Multifunctional Biomaterials for Medicine, Teltow, Berlin, Germany

<sup>⊥</sup>Karlsruhe Nano Micro Facility (KNMF), Karlsruhe Institute of Technology (KIT), 76344 Eggenstein-Leopoldshafen, Germany

## Supporting Information

**ABSTRACT:** In the fields of surgery and regenerative medicine, it is crucial to understand the interactions of proteins with the biomaterials used as implants. Protein adsorption directly influences cell-material interactions *in vivo* and, as a result, regulates, for example, cell adhesion on the surface of the implant. Therefore, the development of suitable analytical techniques together with well-defined model systems allowing for the detection, characterization, and quantification of protein adsorbates is essential. In this study, a protocol for the deposition of highly stable, thin gelatin-based films on various substrates has been developed. The hydrogel films were characterized morphologically and chemically. Due to the obtained low thickness of the hydrogel layer, this setup allowed for a quantitative study on the interaction of human proteins (albumin and fibrinogen) with the hydrogel by Quartz Crystal Microbalance with Dissipation Monitoring (QCM-D). This technique enables the determination of adsorbant mass and changes in the shear modulus of the hydrogel layer upon adsorption of human proteins. Furthermore, Secondary Ion Mass Spectrometry and principal component analysis was applied to monitor the changed composition of the topmost adsorbate layer. This approach opens interesting perspectives for a sensitive screening of viscoelastic biomaterials that could be used for regenerative medicine.



## 1. INTRODUCTION

Regenerative therapies are a relatively new concept in biomedicine. The underlying approach proposes the curing of various diseases by regenerating nonfunctioning cells, diseased tissues or organs via biological substitution, for example by using cultured tissue from an *ex vivo* source or via stimulation of the patient's regenerative processes.<sup>1</sup> Recent studies showed encouraging results in striving for more and more complex systems substituting damaged tissues. For this purpose, biomimetic materials are often used as scaffolds, providing a suitable microenvironment for preseeded and the host's cells to induce tissue regeneration and to avoid implant encapsulation.<sup>2</sup> For example, gelatin has been chosen in many studies since it is obtained by partial hydrolysis and denaturation of collagen, the most abundant component of the extra cellular matrix. Gelatin is nontoxic, biocompatible, biodegradable, and nonimmunogenic.<sup>3–7</sup> Produced in large quantities from bones, skin and tendons of animals such as porcine or cattle,<sup>8</sup> this material serves in medicine as a coating of implants,<sup>9–12</sup> as wound dressing,<sup>13–15</sup> as scaffolds for stem cell cultures,<sup>16–18</sup> and as a sustained release matrix for drugs.<sup>19</sup> In this context, gelatin type A-based hydrogels cross-linked with diisocyanates<sup>20</sup> have shown potential for biomedical applications. They possess suitable mechanical properties for soft tissue replacement, such as a shear modulus of 1–20 kPa, as determined by rheology.<sup>21</sup>

Furthermore, these hydrogels are easy to handle, show no cytotoxicity, and are free of endotoxin contamination, biodegradable with adjustable properties and support growth, and survival of human mesenchymal stem cells.<sup>22</sup>

The interaction of biomaterials with biomolecules, in particular proteins, is of crucial importance to use a material as implant into human or animal bodies.<sup>23</sup> As soon as the material gets into contact with interstitial fluid, blood, cells, and ECM, the adsorption of proteins and other biomolecules starts,<sup>24</sup> and the interaction with leucocytes as well as cell adhesion is strongly influenced, which can be an initial step for implant encapsulation.<sup>25,26</sup> Although the resulting composition of the adhesion layer is highly interesting for the healing induced by the implant, only few methods are available to monitor the formation of these adhesion layers, to determine their composition and to answer the question to which extent the adlayer composition is constant or changes as a function of time,<sup>27</sup> which is especially relevant for degradable materials. Time-dependent studies on protein adsorption have been reported for model surfaces using for example Surface Plasmon Resonance (SPR) spectroscopy or Quartz Crystal Microbalance with Dissipation monitoring (QCM-D).<sup>28–30</sup> Few studies deal

Received: January 25, 2014

Published: June 23, 2014

with protein/hydrogel interaction monitored in situ and as a function of time by QCM-D.<sup>31,32</sup> For example, van Vlierbergh et al. evaluated the interaction between a bovine gelatin-based hydrogel and fibronectin by combining SPR, QCM, and radiolabeling.<sup>33</sup> However, in this study no dissipation monitoring was performed and, therefore, mechanical properties of the interaction from the protein with the hydrogel thin films being crucial for the performance as a biomaterial were not determined. Recently, via coupling of QCM-D with a subsequent MALDI-ToF analysis, it could be demonstrated that the composition of protein-adsorbed layers after applying mixed protein solutions show pronounced time dependencies.<sup>34</sup> In any case, well-defined model surfaces are essential for studies using SPR and QCM-D. Examples are thiolate-based self-assembled monolayers (SAMs) on Au substrates, which allow the investigation of the interaction of proteins with the organic surfaces in a straightforward fashion.<sup>35–38</sup> However, a key requirement for this method is that the organic layer serving as the substrate for protein adsorption does not exceed a thickness of about 100 nm in swollen state; otherwise, the high sensitivity of the QCM-D technique is significantly decreased.

The generation of such thin, well-defined films is especially challenging for covalently cross-linked (bio)polymer-based hydrogels exhibiting a 3D network structure. The chemical cross-linking and the deposition of the hydrogel need to be performed on a substrate as the shape of the formed specimens cannot be altered afterward. In the case of protein-based materials, protein adsorption studies are furthermore difficult because of the inherent similarity of the proteinaceous substrate material and the adsorbant, precluding the use of general protein-sensitive methods. As labeling of proteins might influence their adsorption behavior, a label-free method would be beneficial.

Based on the pioneering works of Wagner and co-workers,<sup>39</sup> today Time-of-Flight Secondary Ion Mass Spectrometry (ToF-SIMS) combined with principal component analysis is used as a powerful tool to study protein adsorbates; for a review, see ref 40. These studies were initially applied to pure adsorbates of one protein at a time onto a chemically inert surface (mica, gold). Later developments and experiments broadened the application of SIMS and PCA toward chemically reactive substrates introducing additional orientation effects in the adsorbate,<sup>41</sup> being of great importance for antibody adsorption, binary mixtures of proteins competing for adsorption,<sup>42</sup> or even corresponding proteins from different species.<sup>39</sup> It was concluded that the differentiation of two proteins based on PCA of SIMS data is feasible as long as the concentration ratio exceeds 10/90 in adsorbed binary mixtures or if the amino acid difference between two proteins is >10%.

In the present study, we address these challenges by reporting the fabrication of stable, thin, gelatin-based hydrogel films, inspired by a previous study,<sup>20</sup> describing an original synthesis of hydrogel films with a thickness in the range from 1 to 3 nm in the swollen state. A particularly important development consisted in the scale decrease of the produced material: from the macro-hydrogel studied by Tronci et al.<sup>20</sup> to hydrogel films of a few tens of nanometers (to fit with QCM-D requirements), which required a new synthesis protocol. After characterizing these gelatin-based model surfaces by ellipsometry, Atomic Force Microscopy (AFM) and Infrared Reflection Absorption Spectroscopy (IRRAS), we investigated the interaction of human serum albumin (HSA) and human fibrinogen (Fbn) on these films by QCM-D and Time-of-Flight

Secondary Ion Mass Spectrometry (ToF-SIMS) in order to quantify the interaction of proteins with a protein-based material by a label-free method.

## 2. MATERIALS AND METHODS

**Materials.** Gelatin from porcine skin (type A; gel strength ~175 bloom), phosphate buffered saline tablets (PBS; 0.01 M phosphate buffer), 3-(trimethoxysilyl)propyl methacrylate 98%, Tween 20, and fibrinogen from human plasma were purchased from Sigma-Aldrich Chemie GmbH Taufkirchen, Germany. Anhydrous dimethylformamide (DMF) was obtained from VWR International GmbH Bruchsal, Germany. Human serum albumin (HSA; fraction V, high purity) and sodium dodecyl sulfate (SDS) was purchased from Merck KGaA Darmstadt, Germany. Hellmanex II solution (1 vol % solution in water) was bought from Hellma, Müllheim, Germany. L-Lysin diisocyanate ethyl ester (LDI) was obtained from Yipeng Chemical Co., China, and was distilled prior to use. Ultrapure water from a Milli-Q plus system (Millipore, Schwalbach, Germany) was used for the preparation of buffer, protein, and gelatin solutions. Silicon wafers were obtained from Silicon Materials, Kaufering, Germany. When used as Si substrates, wafers were first silanized with 3-(trimethoxysilyl)propyl methacrylate. When used to produce gold wafers, they were sputtered with 5 nm titanium and 100 nm gold. QCM-D sensor crystals with top gold electrode (gold-coated AT-cut quartz crystals, QSX301, 5 MHz) were purchased from Q-Sense AB, Göteborg, Sweden.

**Fabrication of Thin Gelatin-Based Hydrogel Films.** A thin film of poly(4-aminomethyl-*p*-xylylene-*co*-*p*-xylylene) was first coated on the substrates (silicon wafers, QCM-D sensor crystals or gold wafers) via chemical vapor deposition (CVD) polymerization to improve subsequent hydrogel anchoring on the surface. CVD polymerization of 4-aminomethyl[2.2]paracyclophane has been adapted from a protocol described in a previous study,<sup>43</sup> at a pyrolysis temperature of 660 °C.

Gelatin (1 wt %) was dissolved in water under magnetic stirring at 55 °C. A clear solution was obtained after approximately 30 min. The deposition of thin films on CVD-modified Au or Si substrates was then carried out by spin-coating (spin processor WS-650 23 NPP Series; S/N 12820; Laurell Technologies Corporation, North Wales, U.S.A.). A two-step process was used. In the first step, the aqueous gelatin solution was deposited on the substrate while using low acceleration (500 rpm/s) and speed (1000 rpm) for 5 s, and in the second step, a thin and dry film was obtained by using high acceleration (4 200 rpm/s) and speed (12 000 rpm) for 60 s. Cross-linking of the gelatin chains has been performed by immersing the substrate for 60 min in an LDI solution (10 mM in DMF) under an argon atmosphere (approximately 7 μM LDI/1 ng gelatin). This process yields a stable, thin hydrogel film. The substrates, coated with the gelatin-based hydrogel, were washed for 30 min at 37 °C in Millipore water.

**Morphological Characterization of Thin Gelatin-Based Hydrogel Films.** Thickness of the different dry coatings was measured by ellipsometry using a multiwavelength rotating analyzer ellipsometer (J. A. Woollam M-44, wavelength range 400–800 nm, J.A. Woollam Co., Inc., Lincoln NE, U.S.A.) at an incident angle of 75° to the surface. The evaluation of the data was performed with the WVASE32 software applying stratified layer optical model, taking into account the substrate and an organic layer, where the real part of the refractive index was described using a Cauchy dispersion line shape. Each sample was measured three times on different areas and the average value was calculated.

Atomic Force Microscopy (AFM) was performed with an Asylum Research Atomic Force Microscope, MFP-3D BIO (Santa Barbara, U.S.A.). The substrates were scanned at 25 °C in air in an isolated chamber, in alternating current mode (AC mode). NSC-18 AFM-HQ cantilevers (Nano&more GmbH Wetzlar, Germany) with the following properties were used: nominal resonance frequency of 75 kHz and nominal spring constant of 3.5 N/m.

To measure the reduced E-modulus of the cross-linked gelatin-based films MLCT shape C tips with a spring constant of 24.20 pN/nm (Nano&more GmbH Wetzlar, Germany) were used. Ten

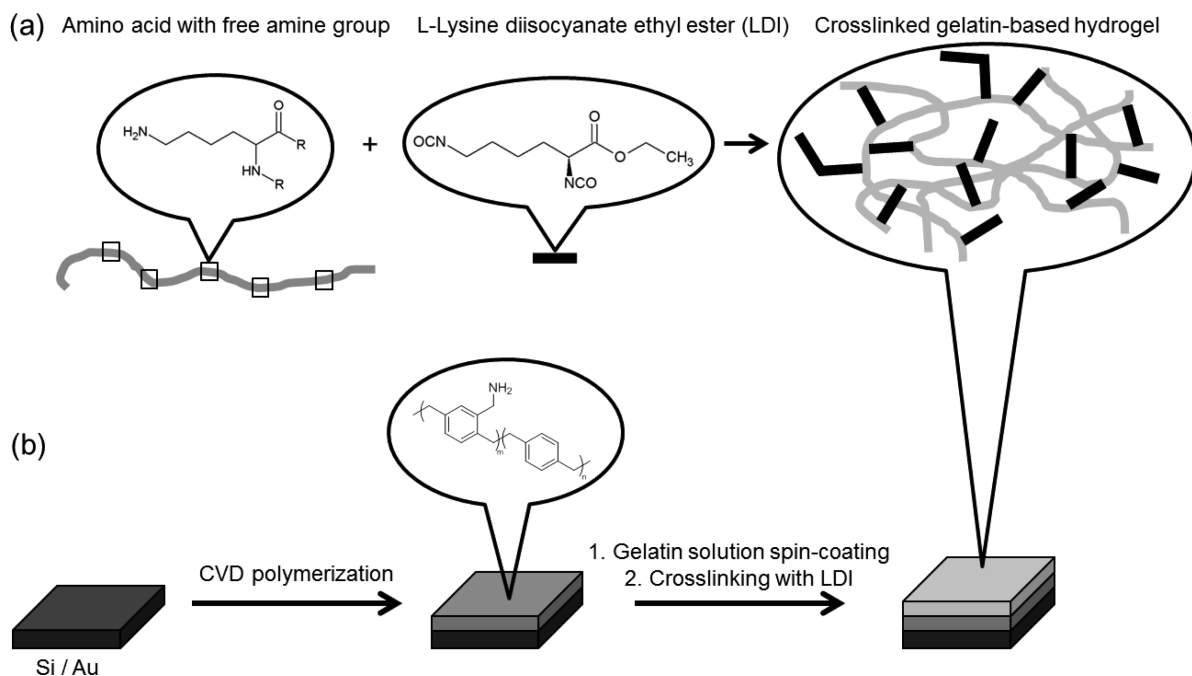


**Figure 1.** Fabrication of thin gelatin-based hydrogel films: chemical structures (a) and fabrication process of the cross-linked film (b).

indentations at each data point were recorded at 0.2 Hz scan rate at 25 and 37 °C, respectively. Samples were submerged in Millipore water.

**Quantitative Characterization of Protein Interaction with Thin Gelatin-Based Hydrogel Films.** Quartz Crystal Microbalance with Dissipation monitoring (QCM-D) experiments were carried out using a Q-Sense E4 instrument with QSoft 401 software (Q-Sense AB, Göteborg, Sweden). Gold-coated quartz crystals were used to analyze protein adsorption on the different coatings. Before any measurement, Hellmanex II solution followed by distilled water and PBS buffer (0.01 M phosphate buffer) were used to rinse QCM-D tubings. The quartz crystal oscillated in the thickness-shear mode at its fundamental resonance frequency of approximately 5 MHz and several overtones. The driving voltage was periodically switched on and off, and the decaying signal was recorded and fitted with a damped oscillation.<sup>44</sup>

Protein adsorption was measured after establishment of a stable frequency and dissipation baseline, in PBS buffer, at a flow rate of 50  $\mu\text{L}/\text{min}$  (ISM 597, Ismatec, Wertheim, Germany) while keeping the QCM-D cell at 37 °C. For HSA and fibrinogen adsorption measurements, protein solutions with a concentration of 1 mg/mL in PBS at pH 7.4 were chosen. At the end of the measurements, the system was rinsed with buffer solution under the same conditions to remove loosely attached proteins from the sensors. The evaluation of the data was performed with the Qtools software (Q-Sense). The layer thickness and wet mass of adsorbed proteins were calculated by using the Voigt viscoelastic model. Therein, resonance frequency variation,  $\Delta f$ , and energy dissipation variation,  $\Delta D$ , data were fitted at the third, fifth, and seventh overtones to calculate the wet mass of adsorbed proteins and viscoelastic properties.<sup>45</sup> QCM-D cells were finally cleaned in an ultrasonic bath at 40 °C with an aqueous solution containing 2.0 vol % SDS and 0.1 vol % Tween 20, washed three times with Ultrapure water from a Milli-Q plus system, and dried with nitrogen.

**Chemical Characterization of Thin Gelatin-Based Hydrogel Films.** For Infrared Reflection Absorption Spectroscopy (IRRAS) measurements, a Vertex 80 FT-IR spectrometer with an 80° grazing incidence specular reflectance accessory (Bruker Optics, Ettlingen, Germany) was used. The samples were measured in the dry state. For the reference measurements, 1024 scans were collected. A fully deuterated hexadecanethiol SAM, prepared on a gold substrate, was used as the reference sample. Dry air was continuously purged through the spectrometer and the sample compartment. Samples were

measured as long as the water absorption bands from ambient air disappeared (1200–1700 scans).

ToF-SIMS (Time-of-Flight Secondary Ion Mass Spectrometry) was performed on a TOF.SIMS5 instrument (ION-TOF GmbH, Münster, Germany) equipped with a Bi cluster primary ion source and a reflectron type time-of-flight analyzer. Ultrahigh vacuum base pressure was below  $5 \times 10^{-9}$  mbar. For high mass resolution, the Bi source was operated in the “high current bunched” mode, providing  $\text{Bi}_3^+$  primary ion pulses at 25 keV energy and a lateral resolution of approximately 4  $\mu\text{m}$ . The short pulse length of 1.0 to 1.2 ns allowed for high mass resolution ( $m/\Delta m > 4000$ ). The primary ion beam was rastered across a  $500 \times 500 \mu\text{m}^2$  field of view on each sample, and  $128 \times 128$  data points were recorded. Primary ion doses were kept below  $10^{11}$  ions/ $\text{cm}^2$  (static SIMS limit). Spectra were calibrated on the omnipresent  $\text{C}^-$ ,  $\text{C}_2^-$ , and  $\text{C}_3^-$  or on the  $\text{C}^+$ ,  $\text{CH}^+$ ,  $\text{CH}_2^+$ , and  $\text{CH}_3^+$  peaks. Protein adsorbate characterization was performed on the gelatin-coated QCM-D sensor crystals within 24 h after each QCM-D experiment. After the QCM-D runs, samples were rinsed with Millipore water, dried, and stored cool and dark. For the principal component analysis of the protein data recorded in positive polarity, the data sets were split in four fields of  $250 \times 250 \mu\text{m}^2$  each and peak lists containing characteristic amino acid side chain fragments<sup>46</sup> were computed. The peak intensities were normalized to the sum of the signals of the individual data sets and square root mean centered. Principal component analysis was performed using a software package for Matlab (MathWorks, Natick, Massachusetts, U.S.A.) provided by D. Graham.<sup>47</sup> Statistical analysis is based on the method described by Wagner et al.<sup>39</sup>

### 3. RESULTS AND DISCUSSION

**Fabrication of Stable, Thin, Gelatin-Based Hydrogel Films.** To obtain gelatin-coated quartz sensors for subsequent protein adsorption measurements, we developed a new protocol inspired by the synthesis reported for the production of thick gelatin hydrogels (macroscale) by Tronci.<sup>20</sup> Briefly, a cross-linking reaction was performed between free amine groups of individual gelatin chains and LDI, a bifunctional diisocyanate, forming urea bonds. Due to possible hydrolysis of the diisocyanate, also oligomeric cross-links and grafted side chains are likely formed, see Figure 1. To fabricate thin

hydrogel films (nanoscale), required for QCM-D studies, a diluted aqueous solution of gelatin was spin-coated onto the substrate and the obtained coating was then dipped into the LDI solution to cross-link gelatin. Depending on the nature of the substrate and on subsequent operating conditions (biological environment), covalent bonding of the hydrogel to the substrate may be necessary. The adhesion of the hydrogel film was guaranteed by prefunctionalizing the substrate via chemical vapor deposition (CVD) polymerization. Poly(4-aminomethyl-*p*-xylylene-*co-p*-xylylene) was deposited on the substrate to obtain a reactive polymer layer, providing free amine groups (ToF-SIMS analysis, see Supporting Information, Figure SI-1). As measured by ellipsometry, a 15 to 20 nm thick polymer coating was deposited on the substrate by CVD polymerization. Subsequently, spin-coating of a 1 wt % gelatin solution deposited a hydrogel film of  $15 \pm 1$  nm thickness (dry state). Cross-linking with LDI enabled the immobilization of gelatin on the CVD substrate (Figure 1). Even after washing, the cross-linked gelatin-based hydrogel film remained on the substrate. Hydrogel film thickness in the hydrated state is estimated to 35–40 nm, which corresponds to a degree of swelling of 230–270 vol %. In contrast, non-cross-linked gelatin films were removed by washing (remaining thickness of  $1.5 \pm 1$  nm on the CVD coating, and remaining thickness close to zero on pure silicon substrate). Exposing the cross-linked gelatin layers to a 10 M urea solution containing 0.1% SDS, pH 3.4, resulted in no film thickness decrease, as monitored by QCM-D and *ex situ* ellipsometry. Indentation by AFM was used to determine the reduced elastic modulus  $E_r$ . Values of  $E_r = 27 \pm 3$  kPa to  $174 \pm 51$  kPa were determined at 25 °C, depending on the indentation force (8 nN to 1 nN). Lower  $E_r$  values were determined at 37 °C ( $18 \pm 2$  to  $106 \pm 19$  kPa), which can be rationalized by a stabilization of the hydrogel through triple helical regions of the gelatin, which disentangle upon heating. This corresponds to the behavior of bulk materials received from LDI cross-linking of gelatin. Furthermore, the mechanical data corroborate the cross-linking in addition to the grafting of the gelatin to the substrate, as in the latter case at 37 °C much lower  $E_r$  values would have been anticipated.

**Characterization of Thin Gelatin-Based Hydrogel Films.** As previously mentioned, film thicknesses of the CVD polymer ( $15\text{--}20 \pm 1$  nm) and the hydrogel film ( $15 \pm 1$  nm) were measured after each preparation step by ellipsometry at room temperature. These results were confirmed by Atomic Force Microscopy (AFM). Via this technique, the roughness and the height of the dry gelatin-based thin film on the CVD-modified surface were measured by scratching the sample. The sample was lightly scratched using a pair of tweezers, applying not enough force to damage the surface of the silicon wafer, thus, ensuring that only the hydrogel and the CVD modification is removed. Figure 2 shows a  $20 \mu\text{m}$  topography scan of the scratched film and the recorded profile. The average roughness was equal to 1 nm and the total height was approximately 30 nm, as expected.

Infrared Reflection Absorption Spectroscopy (IRRAS)<sup>48</sup> was used to check the chemical composition of the surface layers. Cross-linked and non-cross-linked gelatin-based films on amino-functionalized substrates were analyzed. Figure 3 shows that, even after intensive washing, the cross-linked gelatin hydrogel film remains on the surface, previously modified with amino-functionalized CVD polymer. Indeed, the broad hydroxyl band at  $\sim 3500$   $\text{cm}^{-1}$  and amide bands I to III at  $\sim 1600$   $\text{cm}^{-1}$  on spectrum 4 indicate the presence of the

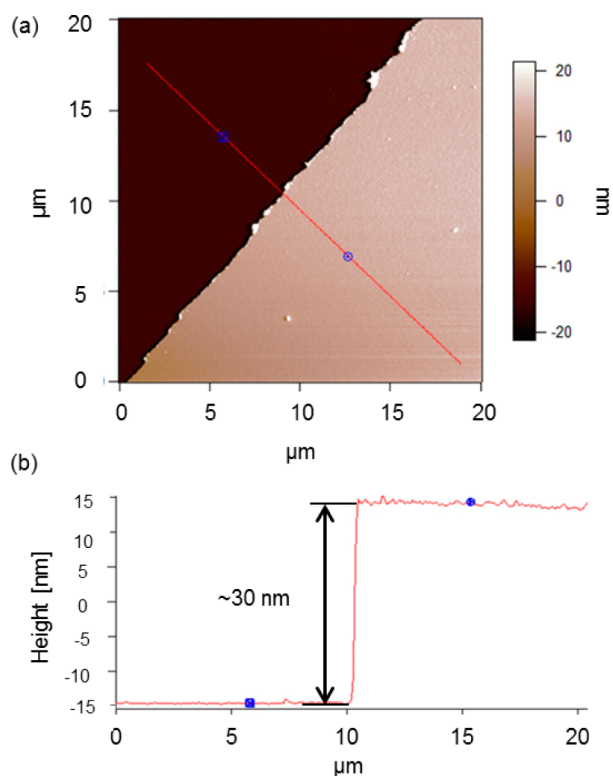


**Figure 2.** AFM-based  $20 \mu\text{m}$  topography scan of a scratched cross-linked gelatin-based thin film on a CVD polymer (a) and recorded profile (b) along the red line.

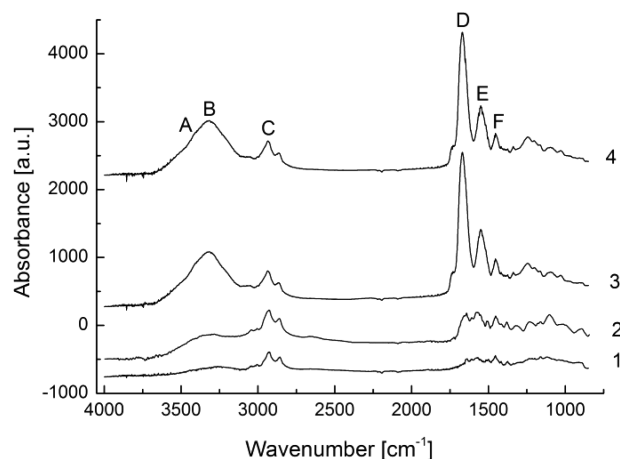


**Figure 3.** IRRAS spectra of the amino-functionalized CVD polymer (1), coated with non-cross-linked gelatin after washing (2), or coated with cross-linked gelatin prior to washing (3) and after washing (4).

protein on the surface. If, however, the cross-linking step is omitted (see spectrum 2), the majority of the deposited gelatin is removed from the surface by washing at 37 °C. The absence of a band at  $\sim 2250$   $\text{cm}^{-1}$  indicates that the isocyanate groups were completely converted.<sup>21</sup> Assignments of bands ascribed to gelatin, in accordance with a previous study,<sup>49</sup> are given in Supporting Information, Table SI-1.

**Quantitative Characterization of Protein/Hydrogel Interaction Measured by QCM-D.** For quantitative protein/hydrogel interaction studies using the QCM-D technology, very thin gelatin films ( $<100$  nm, swollen state) are mandatory to avoid strong damping of the shear wave

oscillation by viscoelastic losses within the hydrogel layer. These requirements are met by the gelatin films produced via the reported protocol. Therefore, the protein/hydrogel interaction can be investigated by QCM-D, where the resonance frequencies ( $\Delta f$ ) and the energy dissipations ( $\Delta D$ ) are recorded during the protein adsorption process. The resonance frequencies decrease with increasing mass of adsorbed protein ( $m$ ) per area ( $A$ ). The wet protein mass on the sensor crystal was calculated from frequency and dissipation data applying the Voigt model.<sup>45,50</sup> The frequency and dissipation shift during Fbn adsorption on three different coatings (gelatin, gold, CVD polymer) at the third overtone is shown in Figure 4. The corresponding calculated wet masses of

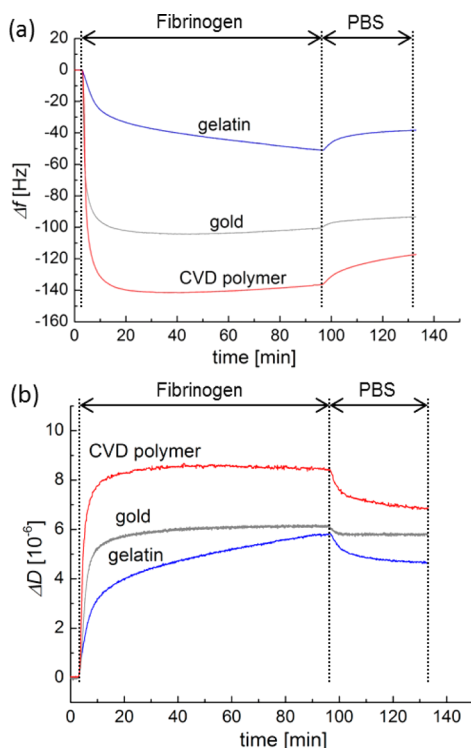


**Figure 4.** Frequency shifts (a) and dissipation shifts (b) during Fbn adsorption on CVD coating (red), bare gold (gray), and gelatin-based hydrogel (blue) at 3rd overtone ( $f = 15$  MHz) at 37 °C in the QCM-D study. The according frequency shift and dissipation shift over time for HSA is shown in the Supporting Information, Figure SI-2.

the adsorbed proteins (HSA or Fbn) determined by the Voigt model are displayed in Figure 5. The adsorption of human protein at the surface of the gelatin-based hydrogel ( $7.9 \pm 0.8$  mg/m<sup>2</sup>,  $n = 13$ , for Fbn, and  $0.4 \pm 0.1$  mg/m<sup>2</sup>,  $n = 8$ , for HSA) was much lower than at the CVD-modified surface and gold ( $35.8 \pm 0.9$  mg/m<sup>2</sup>,  $n = 7$ , and  $18.1 \pm 1.0$  mg/m<sup>2</sup>,  $n = 5$ , respectively, for Fbn, and  $11.4 \pm 1.3$  mg/m<sup>2</sup>,  $n = 12$  and  $12 \pm 1.6$  mg/m<sup>2</sup>,  $n = 5$ , respectively, for HSA). All experiments were repeated several times. The standard deviations of the results of the individual experiments are indicated by the error bars in Figure 5. It has to be noted that the statistical deviations are very low and that the experiments are well reproducible. Compared to reported results on fibrinogen adsorbed on gold under similar conditions,<sup>51</sup> our obtained values for  $\Delta D$  and  $\Delta f$  lie in the expected range. Actually the absorbed amounts of Fbn and HSA were close to the amounts reported for PEG-modified surfaces ( $0.5$ – $1.0$  mg/m<sup>2</sup> for HSA and  $1.0$ – $2.0$  mg/m<sup>2</sup> for

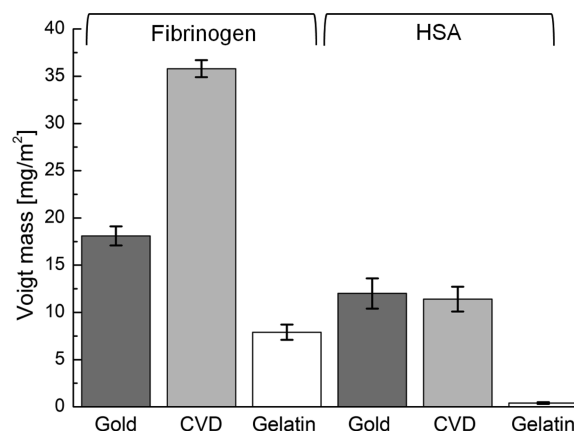


**Figure 5.** Adsorbed wet mass of Fbn on bare gold (dark gray), CVD (light gray), and gelatin film (white) calculated with the Voigt model from QCM-D measurements performed at 37 °C.

Fbn)<sup>52</sup> but still much higher than optimized PEG-based protein resistant surfaces ( $<0.01$  mg/m<sup>2</sup> for HSA and  $\sim 0.01$ – $0.30$  mg/m<sup>2</sup> for Fbn).<sup>26,53</sup>

In Figure 6, the dissipation shift is plotted versus the frequency shift. A linear relationship between the dissipation

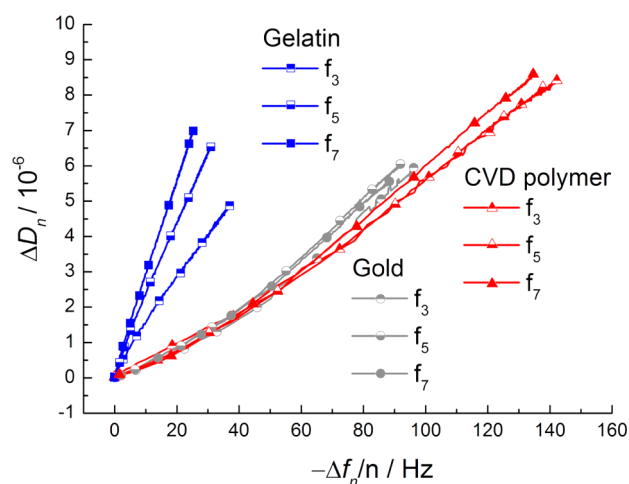


**Figure 6.**  $\Delta D_n/(-\Delta f_n)$  values during the adsorption process of Fbn on the gelatin-based hydrogel (blue shades; squares), on bare gold (gray shades; circles), and on the CVD polymer (magenta shades; triangles). The corresponding  $\Delta D_n/(-\Delta f_n)$  plot for HSA is shown in the Supporting Information, Figure SI-3. For the sake of clarity, only the third, fifth, and seventh resonance frequencies are shown.

shift and the frequency shift is clearly visible. For all samples, the factors of proportionality,  $\Delta D_n/(-\Delta f_n)$ , for the fifth overtone are shown in Table 1. This linear relationship allows the determination of the shear modulus ( $G_f$ ) of the thin adsorbed protein layer, as described by eq 1 (see Supporting Information<sup>54</sup>):

$$G_f = \frac{4\pi\eta}{\Delta D_n/(-\Delta f_n)} \quad (1)$$

From the similar  $\Delta D/\Delta f$  behavior (determined shear moduli for fifth overtone are shown in Table 1) of samples on CVD polymer and gold, shown in Figure 6, it follows that the fibrinogen films exhibit similar viscoelastic properties on these substrates. However, the corresponding data for fibrinogen

**Table 1.**  $\Delta D_s/(-\Delta f_s)$  and Shear Moduli ( $G_f$ ) of the Adsorbed Protein Layer on Various Substrates Determined by Eq 1<sup>a</sup>

substrate		$\Delta D_s/(-\Delta f_s)$ [ $10^{-6}$ s]	$G_f$ [kPa]
HSA	Au ( $n = 5$ )	$0.172 \pm 0.009$	$51.2 \pm 2.6$
	CVD polymer ( $n = 13$ )	$0.168 \pm 0.03$	$53.8 \pm 9.0$
	gelatin hydrogel ( $n = 6$ )	$0.37 \pm 0.12$	$25.9 \pm 8.3$
Fbn	Au ( $n = 5$ )	$0.065 \pm 0.007$	$137.0 \pm 15.0$
	CVD polymer ( $n = 7$ )	$0.062 \pm 0.001$	$143.1 \pm 2.2$
	gelatin hydrogel ( $n = 13$ )	$0.2 \pm 0.048$	$46.4 \pm 10.9$

<sup>a</sup>Bar diagram with standard deviation, see Supporting Information, Figures SI-5 and SI-6.

interacting with the immobilized gelatin hydrogel are clearly different. This observation pinpoints the hypothesis of fibrinogen entering the gelatin gel, leading also to new viscoelastic properties of this new two-component gel. Scrutinizing this effect, we performed a kinetic analysis of the QCM-D data (see Figure SI-4). A two-step kinetic behavior for fibrinogen interacting with gelatin (but not for the inert substrates) was found. In all cases, a rapid initial exponential  $\Delta f$  decrease was found (time constants of approximately 150 s). Only in the case of the gelatin substrate, this first step was followed by a second, much slower, process (time constant 3300 s). During this phase, the  $\Delta f$  changed further. This observation corroborates with the reasonable hypothesis of proteins slowly entering the gelatin layer, leading to the second 20% of the overall frequency drop. From the lower shear modulus of the protein-loaded hydrogel (higher  $\Delta D_n/(-\Delta f_n)$  ratio) and the lesser wet protein mass detected on gelatin, it can be concluded that the proteins interacting with the gelatin substrates are less densely packed as compared to proteins on gold respectively CVD coating. A less densely packed protein layer indicates a minor interaction of the proteins with the gelatin-based hydrogel<sup>26</sup> and might lead to a lower risk of rejection of the implant and better biocompatibility and hemocompatibility, although additional effects of a multitude of other parameters have to be taken into account to predict possible consequences, depending on the particular in vivo situation.

In general, the shear moduli determined by QCM-D are in good agreement with the shear modulus of viscoelastic polymer materials calculated by Voinova.<sup>45</sup>

**Characterization of Protein/Hydrogel Interaction on Thin Hydrogel Films by ToF-SIMS.** Protein solutions, prepared from human Fbn or albumin in PBS, were flushed on gelatin-based hydrogel thin film-coated QCM-D sensors (37 °C, 1 mg/mL). Advanced chemical characterization of the adsorbed protein layers on gelatin hydrogels has been performed by ToF-SIMS. Such experiments could not be carried out by IRRAS, since the latter would not enable the distinction between different proteins. ToF-SIMS measurements were thus performed to characterize the topmost layer of thin gelatin-based hydrogel film (sampling depth of static SIMS is only 2–5 nm), exposed to human proteins. Under primary ion bombardment, proteins decompose yielding characteristic fragments of the amino acid side chains. Since the signal intensities of the amino acids fragments define a multivariate data set (for a detailed peak list, see Table SI-2 in Supporting Information), principal component analysis was applied to reduce data dimensionality and complexity. Using principal

component analysis, we can discern between pure gelatin surfaces and those loaded with Fbn or albumin. Studies of Muramoto<sup>55</sup> and Tyler<sup>56</sup> have been addressing other sets of proteins. Figure 7a shows the clustering of the obtained data in

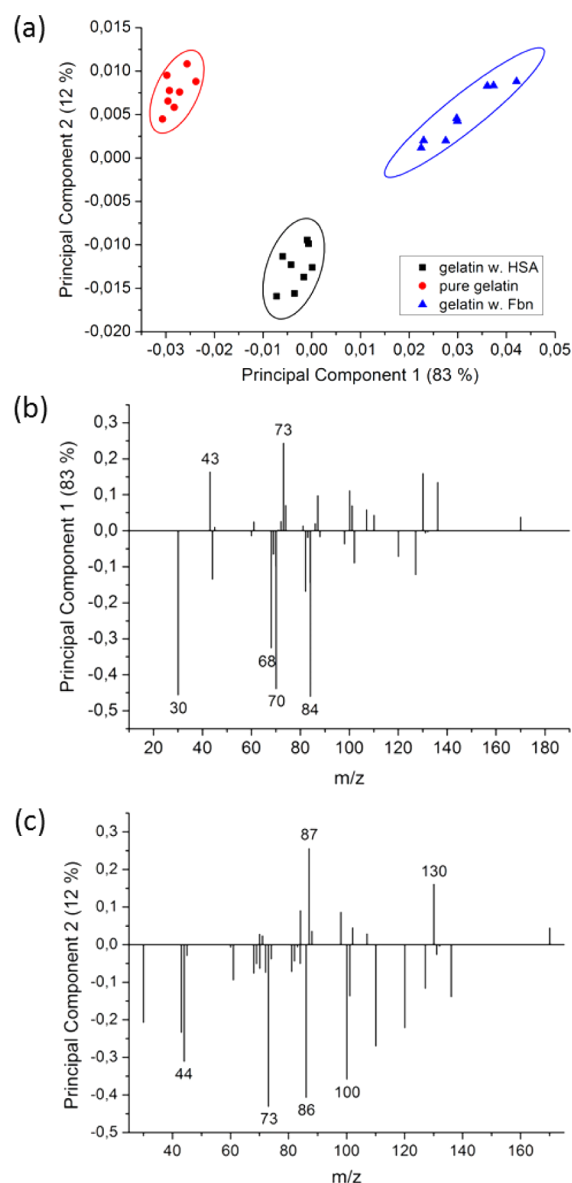


**Figure 7.** Scores of PC1 (83% variance) and PC2 (12% variance) from three different experiments ( $n = 24$ ), together with 95% confidence limits (a); loadings of PC1 (b); loadings of PC2 (c). For details, see SI.

the principal component analysis of the characteristic amino acids fragments. Whereas PC1, capturing 84% of the variance, obviously discriminates well between the pure gelatin surfaces (Figure 7a, circles) and the HSA (squares), respectively, Fbn (triangles) treated gelatin samples; PC2 (12% variance) separates best the HSA-treated samples. As can be seen from the corresponding loading plots, Figure 7b (see also SI), arginine (43, and 73  $m/z$ ) has strong positive loadings for PC1, glycine (30  $m/z$ ), proline (68, and 70  $m/z$ ), and lysine (84  $m/z$ ) have strong negative loadings, nota bene gelatin has negative PC1 score values. These findings are in good accordance with the amino acid compositions of gelatin (see Table SI-3 in Supporting Information)<sup>57,58</sup> since gelatin is rich in glycine and

proline. It should be noted, however, that the  $\text{CH}_4\text{N}^+$  fragment might also arise from other amino acids and leucine and isoleucine both share the SIMS fragment. Therefore, this signal can be misinterpreted. Arginine, alanine, and leucine exhibit strong negative loadings in PC2, Figure 7c. Whereas HSA is indeed richer in isoleucine and leucine as Fbn and gelatin, the reasons for the predominance of arginine and alanine in PC2 are less obvious. These effects are not fully understood today; they can be due to the spatial arrangement of the detected amino acids affecting the sputter yields during the SIMS process (that is also influenced by the primary ion species<sup>55</sup>), or due to side effects of the protein structure affecting ionization probabilities.

Despite the fact that the amounts of adsorbed fibrinogen and albumin were very low on the gelatin samples as compared to, for example, gold surfaces (fibrinogen 44%, HSA 3%). Secondary Ion Mass-Spectrometry in combination with principal component analysis was able to differentiate between these three proteinaceous surfaces. This study demonstrated that SIMS and PCA can also be applied to follow the interaction of proteins from solution with an immobilized and cross-linked gelatin film on a substrate. It should be noted that the passivation effect of the gelatin layer reduced the HSA adsorption strongly, as compared to Wagner et al.,<sup>42</sup> by more than 1 order of magnitude (approximately 5 mg/m<sup>2</sup> dry mass on mica determined from <sup>125</sup>I-labeling vs 0.4 mg/m<sup>2</sup> wet mass from QCM-D). However, PC1 and PC2 captured clearly the differences in amino acid signals, as shown in Figure 7.

#### 4. CONCLUSION

We developed an original method for the fabrication of nanoscopic thin films made of gelatin-based hydrogels that enables precise characterization of protein/hydrogel interactions by QCM-D, a technology limited to thin coatings allowing for the propagation of shear wave oscillations from the quartz crystal through the adlayer(s). The gelatin hydrogels were found to be stable even if exposed to harsh solubilizing solutions containing urea and a detergent. The production of these films is based on a CVD polymer carrying amine groups as supporting layer, which can be deposited independently from the nature of the substrate. Therefore, our approach can be used on any type of material. The amine groups from the polymer increase the stability of the coated gelatin hydrogel since diisocyanates, used to cross-link the gelatin chains, also react with amine groups from the polymer layer. The obtained thin films allowed the quantification of the interaction of two human plasma proteins, HSA and Fbn, with the hydrogel film by QCM-D experiments. The results of these measurements showed that protein interaction with the investigated gelatin-based hydrogels was much lower than with CVD-coated surfaces and also pure gold. Furthermore, shear moduli describing the viscoelastic properties of the protein-loaded hydrogels, can be calculated from the QCM-D data.

The presented data based on several surface analytical methods, demonstrate that despite the different synthesis conditions the nanoscopic films synthesized in DMF are a suitable model for the macroscopic hydrogels synthesized in water. Furthermore, ToF-SIMS investigations showed that the presented setup enables to study the adsorption of proteins from solutions on a proteinaceous matrix. In future studies, such methodologies will be of key importance to study the interaction of other biologically relevant proteins with gelatin-

coated substrates, as well as to monitor changes in adsorbed proteins over time (Vroman effect) without labeling.

Therefore, this study offers new perspectives for the design and fast and efficient screening of new types of hydrogels with regard to protein interaction.

#### ■ ASSOCIATED CONTENT

##### Supporting Information

Additional experimental details and analytic results: Surface analysis of poly(*p*-xylylene) and poly(4-aminomethyl-*p*-xylylene-*co-p*-xylylene) by ToF-SIMS. Table of tentative assignments of some bands frequently found in IRRAS spectra of biological materials and measured bands. Quartz crystal microbalance with dissipation monitoring, viscoelastic model, evaluation of  $\Delta D$  and  $\Delta f$ -plot of HSA and calculation of the shear modulus. Plotting of  $\Delta D_n/(-\Delta f_n)$  values during the HSA adsorption process. Detailed characterization of the adsorption kinetic by exponential fitting of recorded  $-\Delta f$  curve. Plotted  $\Delta D/(-\Delta f)$  ratios and shear moduli. Analysis of adsorbed fibrinogen respectively HSA by ToF-SIMS and principal component analysis. Table of amino acid compositions of the studied proteins. This material is available free of charge via the Internet at <http://pubs.acs.org>.

#### ■ AUTHOR INFORMATION

##### Corresponding Author

\*E-mail: [christof.woell@kit.edu](mailto:christof.woell@kit.edu).

##### Notes

The authors declare no competing financial interest.

#### ■ ACKNOWLEDGMENTS

The authors would like to thank Dan Graham, University of Washington, for developing the NESAC/BIO Toolbox used in this study, the NIH supporting the toolbox development by Grant EB-002027, and David Castner, University of Washington, for fruitful discussions on several aspects of protein analysis based on SIMS and PCA. The authors thank the Helmholtz Association for funding of this work through Helmholtz-Portfolio Topic, Technology and Medicine.

#### ■ REFERENCES

- (1) Atala, A. *Principles of Regenerative Medicine*, 2nd ed.; Elsevier, Academic Press: Amsterdam; Boston, 2011; p xix.
- (2) Ratner, B. D.; Bryant, S. J. Biomaterials: Where we have been and where we are going. *Annu. Rev. Biomed. Eng.* **2004**, *6*, 41–75.
- (3) Vlierberghe, S. V.; Cnudde, V.; Dubruel, P.; Masschaele, B.; Cosijns, A.; Paepe, I. D.; Jacobs, P. J.; Hoorebeke, L. V.; Remon, J. P.; Schacht, E. Porous gelatin hydrogels: 1. Cryogenic formation and structure analysis. *Biomacromolecules* **2007**, *8* (2), 331–7.
- (4) Ulubayram, K.; Eroglu, I.; Hasirci, N. Gelatin microspheres and sponges for delivery of macromolecules. *J. Biomater. Appl.* **2002**, *16* (3), 227–41.
- (5) Takei, T.; Sugihara, K.; Yoshida, M.; Kawakami, K. Injectable and biodegradable sugar beet pectin/gelatin hydrogels for biomedical applications. *J. Biomater. Sci., Polym. Ed.* **2013**, *24* (11), 1333–42.
- (6) Kasahara, H.; Tanaka, E.; Fukuyama, N.; Sato, E.; Sakamoto, H.; Tabata, Y.; Ando, K.; Iseki, H.; Shinozaki, Y.; Kimura, K.; Kuwabara, E.; Koide, S.; Nakazawa, H.; Mori, H. Biodegradable gelatin hydrogel potentiates the angiogenic effect of fibroblast growth factor 4 plasmid in rabbit hindlimb ischemia. *J. Am. Coll. Cardiol.* **2003**, *41* (6), 1056–62.
- (7) Tonsomboon, K.; Strange, D. G.; Oyen, M. L. Gelatin nanofiber-reinforced alginate gel scaffolds for corneal tissue engineering. *Conf. Proc. IEEE Eng. Med. Biol. Soc.* **2013**, *2013*, 6671–4.

- (8) Hago, E. E.; Li, X. S. Interpenetrating polymer network hydrogels based on gelatin and PVA by biocompatible approaches: Synthesis and characterization. *Adv. Mater. Sci. Eng.* **2013**, DOI: 10.1155/2013/328763.
- (9) Inoue, M.; Sasaki, M.; Katada, Y.; Fujiu, K.; Manabe, I.; Nagai, R.; Taguchi, T. Poly-(L-lactic acid) and citric acid-crosslinked gelatin composite matrices as a drug-eluting stent coating material with endothelialization, antithrombogenic, and drug release properties. *J. Biomed. Mater. Res. A* **2013**, *101* (7), 2049–57.
- (10) Sirova, M.; Vlierberghe, S. V.; Matyasova, V.; Rossmann, P.; Schacht, E.; Dubrue, P.; Rihova, B. Immunocompatibility evaluation of hydrogel-coated polyimide implants for applications in regenerative medicine. *J. Biomed. Mater. Res. A* **2014**, *102*, 1982–1990.
- (11) Akoum, A.; Marois, Y.; Roy, R.; King, M.; Guidoin, R.; Sigot, M.; Sigot-Luizard, M. F. Use of myxalin for improving vascular graft healing: evaluation of biocompatibility in rats. *J. Invest. Surg.* **1992**, *5* (2), 129–41.
- (12) Zhang, Q.; Tan, K.; Zhang, Y.; Ye, Z.; Tan, W. S.; Lang, M. In situ controlled release of rhBMP-2 in gelatin-coated 3D porous poly(epsilon-caprolactone) scaffolds for homogeneous bone tissue formation. *Biomacromolecules* **2014**, *15* (1), 84–94.
- (13) Razzak, M. T.; Darwis, D.; Zainuddin; Sukirno. Irradiation of polyvinyl alcohol and polyvinyl pyrrolidone blended hydrogel for wound dressing. *Radiat. Phys. Chem.* **2001**, *62* (1), 107–113.
- (14) Yoshii, F.; Zhanshan, Y.; Isobe, K.; Shinozaki, K.; Makuuchi, K. Electron beam crosslinked PEO and PEO PVA hydrogels for wound dressing. *Radiat. Phys. Chem.* **1999**, *55* (2), 133–138.
- (15) Choi, Y. S.; Lee, S. B.; Hong, S. R.; Lee, Y. M.; Song, K. W.; Park, M. H. Studies on gelatin-based sponges. Part III: a comparative study of cross-linked gelatin/alginate, gelatin/hyaluronate and chitosan/hyaluronate sponges and their application as a wound dressing in full-thickness skin defect of rat. *J. Mater. Sci.: Mater. Med.* **2001**, *12* (1), 67–73.
- (16) Binan, L.; Tendey, C.; De Crescenzo, G.; El Ayoubi, R.; Aji, A.; Jolicoeur, M. Differentiation of neuronal stem cells into motor neurons using electrospun poly-L-lactic acid/gelatin scaffold. *Biomaterials* **2014**, *35* (2), 664–74.
- (17) Ponticciello, M. S.; Schinagl, R. M.; Kadiyala, S.; Barry, F. P. Gelatin-based resorbable sponge as a carrier matrix for human mesenchymal stem cells in cartilage regeneration therapy. *J. Biomed. Mater. Res.* **2000**, *52* (2), 246–55.
- (18) Dubrue, P.; Unger, R.; Vlierberghe, S. V.; Cnudde, V.; Jacobs, P. J.; Schacht, E.; Kirkpatrick, C. J. Porous gelatin hydrogels: 2. In vitro cell interaction study. *Biomacromolecules* **2007**, *8* (2), 338–44.
- (19) Tabata, Y.; Nagano, A.; Muniruzzaman, M.; Ikada, Y. In vitro sorption and desorption of basic fibroblast growth factor from biodegradable hydrogels. *Biomaterials* **1998**, *19* (19), 1781–9.
- (20) Tronci, G.; Neffe, A. T.; Pierce, B. F.; Lendlein, A. An entropy-elastic gelatin-based hydrogel system. *J. Mater. Chem.* **2010**, *20* (40), 8875–8884.
- (21) Neffe, A. T.; Gebauer, T.; Lendlein, A. Tailoring of mechanical properties of diisocyanate crosslinked gelatin-based hydrogels. *MRS Online Proc. Libr.* **2013**, 1569.
- (22) Pierce, B. F.; Pittermann, E.; Ma, N.; Gebauer, T.; Neffe, A. T.; Hölscher, M.; Jung, F.; Lendlein, A. Viability of human mesenchymal stem cells seeded on crosslinked entropy-elastic gelatin-based hydrogels. *Macromol. Biosci.* **2012**, *12* (3), 312–321.
- (23) Anderson, J. M. Biological responses to materials. *Ann. Rev. Mater. Res.* **2001**, *31*, 81–110.
- (24) Wei, Q.; Becherer, T.; Angioletti-Uberti, S.; Dzubiel, J.; Wischke, C.; Neffe, A. T.; Lendlein, A.; Ballauff, M.; Haag, R. Protein interactions with polymer surfaces and biomaterials. *Angew. Chem., Int. Ed.* **2014**, DOI: 10.1002/anie.201400546.
- (25) Burmania, J. A.; Stevens, K. R.; Kao, W. J. Cell interaction with protein-loaded interpenetrating networks containing modified gelatin and poly(ethylene glycol) diacrylate. *Biomaterials* **2003**, *24* (22), 3921–30.
- (26) Schmidt, D. R.; Waldeck, H.; Kao, W. J. Protein Adsorption to Biomaterials. In *Biological Interactions on Materials Surfaces*; Puleo, D. A., Bizios, R., Eds.; Springer: New York, 2009; pp 1–18.
- (27) Vogler, E. A. Protein adsorption in three dimensions. *Biomaterials* **2012**, *33* (5), 1201–37.
- (28) Rodahl, M.; Hook, F.; Kasemo, B. QCM Operation in Liquids: An Explanation of Measured Variations in Frequency and Q Factor with Liquid Conductivity. *Anal. Chem.* **1996**, *68* (13), 2219–27.
- (29) Johannsmann, D.; Reviakine, I.; Richter, R. P. Dissipation in films of adsorbed nanospheres studied by quartz crystal microbalance (QCM). *Anal. Chem.* **2009**, *81* (19), 8167–76.
- (30) Speight, R. E.; Cooper, M. A. A survey of the 2010 quartz crystal microbalance literature. *J. Mol. Recognit.* **2012**, *25* (9), 451–73.
- (31) Scott, E. A.; Nichols, M. D.; Cordova, L. H.; George, B. J.; Jun, Y. S.; Elbert, D. L. Protein adsorption and cell adhesion on nanoscale bioactive coatings formed from poly(ethylene glycol) and albumin microgels. *Biomaterials* **2008**, *29* (34), 4481–93.
- (32) Lord, M. S.; Cousins, B. G.; Doherty, P. J.; Whitelock, J. M.; Simmons, A.; Williams, R. L.; Milthorpe, B. K. The effect of silica nanoparticulate coatings on serum protein adsorption and cellular response. *Biomaterials* **2006**, *27* (28), 4856–62.
- (33) Van Vlierberghe, S.; Vanderleyden, E.; Dubrue, P.; De Vos, F.; Schacht, E. Affinity study of novel gelatin cell carriers for fibronectin. *Macromol. Biosci.* **2009**, *9* (11), 1105–15.
- (34) Kirschhofer, F.; Rieder, A.; Prechtel, C.; Kuhl, B.; Sabljo, K.; Woll, C.; Obst, U.; Brenner-Weiss, G. Quartz crystal microbalance with dissipation coupled to on-chip MALDI-ToF mass spectrometry as a tool for characterising proteinaceous conditioning films on functionalised surfaces. *Anal. Chim. Acta* **2013**, *802*, 95–102.
- (35) Liu, J.; Schupbach, B.; Bashir, A.; Shekhah, O.; Nefedov, A.; Kind, M.; Terfort, A.; Woll, C. Structural characterization of self-assembled monolayers of pyridine-terminated thiolates on gold. *Phys. Chem. Chem. Phys.* **2010**, *12* (17), 4459–72.
- (36) Love, J. C.; Estroff, L. A.; Kriebel, J. K.; Nuzzo, R. G.; Whitesides, G. M. Self-assembled monolayers of thiolates on metals as a form of nanotechnology. *Chem. Rev.* **2005**, *105* (4), 1103–69.
- (37) Silin, V.; Weetall, H.; Vanderah, D. J. SPR studies of the nonspecific adsorption kinetics of human IgG and BSA on gold surfaces modified by self-assembled monolayers (SAMs). *J. Colloid Interface Sci.* **1997**, *185* (1), 94–103.
- (38) Kerstan, A.; Ladnorg, T.; Grunwald, C.; Vopel, T.; Zacher, D.; Herrmann, C.; Woll, C. Human guanylate-binding protein 1 as a model system investigated by several surface techniques. *Biointerphases* **2010**, *5* (4), 131–8.
- (39) Wagner, M. S.; Castner, D. G. Characterization of adsorbed protein films by time-of-flight secondary ion mass spectrometry with principal component analysis. *Langmuir* **2001**, *17* (15), 4649–4660.
- (40) Castner, D. G.; Ratner, B. D. Biomedical surface science: Foundations to frontiers. *Surf. Sci.* **2002**, *500* (1–3), 28–60.
- (41) Liu, F.; Dubey, M.; Takahashi, H.; Castner, D. G.; Grainger, D. W. Immobilized antibody orientation analysis using secondary ion mass spectrometry and fluorescence imaging of affinity-generated patterns. *Anal. Chem.* **2010**, *82* (7), 2947–2958.
- (42) Wagner, M. S.; Shen, M.; Horbett, T. A.; Castner, D. G. Quantitative analysis of binary adsorbed protein films by time of flight secondary ion mass spectrometry. *J. Biomed. Mater. Res., Part A* **2003**, *64* (1), 1–11.
- (43) Chen, H. Y.; McClelland, A. A.; Chen, Z.; Lahann, J. Solventless adhesive bonding using reactive polymer coatings. *Anal. Chem.* **2008**, *80* (11), 4119–24.
- (44) Rodahl, M.; Kasemo, B. A simple setup to simultaneously measure the resonant frequency and the absolute dissipation factor of a quartz crystal microbalance. *Rev. Sci. Instrum.* **1996**, *67* (9), 3238–3241.
- (45) Voinova, M. V.; Rodahl, M.; Jonson, M.; Kasemo, B. Viscoelastic acoustic response of layered polymer films at fluid-solid interfaces: Continuum mechanics approach. *Phys. Scr.* **1999**, *59* (5), 391–396.



- (46) Lhoest, J. B.; Wagner, M. S.; Tidwell, C. D.; Castner, D. G. Characterization of adsorbed protein films by time of flight secondary ion mass spectrometry. *J. Biomed. Mater. Res.* **2001**, *57* (3), 432–40.
- (47) Graham, D. J.; Wagner, M. S.; Castner, D. G. Information from complexity: Challenges of TOF-SIMS data interpretation. *Appl. Surf. Sci.* **2006**, *252* (19), 6860–6868.
- (48) Kattner, J.; Hoffmann, H. External Reflection Spectroscopy of Thin Films on Dielectric Substrates. *Handbook of Vibrational Spectroscopy*; Wiley: New York, 2002.
- (49) Naumann, D. FT-infrared and FT-Raman spectroscopy in biomedical research. *Appl. Spectrosc. Rev.* **2001**, *36* (2–3), 239–298.
- (50) Dutta, A. K.; Belfort, G. Adsorbed gels versus brushes: viscoelastic differences. *Langmuir* **2007**, *23* (6), 3088–94.
- (51) Hemmersam, A. G.; Foss, M.; Chevallier, J.; Besenbacher, F. Adsorption of fibrinogen on tantalum oxide, titanium oxide and gold studied by the QCM-D technique. *Colloids Surf., B* **2005**, *43* (3–4), 208–15.
- (52) Sharma, S.; Popat, K. C.; Desai, T. A. Controlling nonspecific protein interactions in silicon biomicrosystems with nanostructured poly(ethylene glycol) films. *Langmuir* **2002**, *18* (23), 8728–8731.
- (53) Kenausis, G. L.; Voros, J.; Elbert, D. L.; Huang, N. P.; Hofer, R.; Ruiz-Taylor, L.; Textor, M.; Hubbell, J. A.; Spencer, N. D. Poly(L-lysine)-g-poly(ethylene glycol) layers on metal oxide surfaces: Attachment mechanism and effects of polymer architecture on resistance to protein adsorption. *J. Phys. Chem. B* **2000**, *104* (14), 3298–3309.
- (54) Du, B.; Johannsmann, D. Operation of the quartz crystal microbalance in liquids: derivation of the elastic compliance of a film from the ratio of bandwidth shift and frequency shift. *Langmuir* **2004**, *20* (7), 2809–12.
- (55) Muramoto, S.; Graham, D. J.; Wagner, M. S.; Lee, T. G.; Moon, D. W.; Castner, D. G. ToF-SIMS analysis of adsorbed proteins: principal component analysis of the primary ion species effect on the protein fragmentation patterns. *J. Phys. Chem. C* **2011**, *115* (49), 24247–24255.
- (56) Tyler, B. J.; Bruening, C.; Ranganathan, S.; Arlinghaus, H. F. TOF-SIMS imaging of adsorbed proteins on topographically complex surfaces with  $\text{Bi}_3^+$  primary ions. *Biointerphases* **2011**, *6* (3), 135.
- (57) Eastoe, J. E. The amino acid composition of mammalian collagen and gelatin. *Biochem. J.* **1955**, *61* (4), 589–600.
- (58) ExPASy - SIB Bioinformatics Resource Portal. <http://www.expasy.org/>.